# Evidence for Singlet-Oxygen Generation and Biocidal Activity in Photoresponsive Metallic Nitride Fullerene-Polymer Adhesive Films

**ARTICLE** *in* ACS APPLIED MATERIALS & INTERFACES · APRIL 2009

Impact Factor: 6.72 · DOI: 10.1021/am900008v · Source: PubMed



**9 AUTHORS**, INCLUDING:

Praveen K Madasu
University of Southern Mississippi
**3** PUBLICATIONS **53** CITATIONS
SEE PROFILE

Preston A Fulmer
United States Naval Research Laboratory
**22** PUBLICATIONS **306** CITATIONS
SEE PROFILE

James H. Wynne
United States Naval Research Laboratory
**58** PUBLICATIONS **479** CITATIONS
SEE PROFILE

Steven Stevenson
Indiana University-Purdue University at Fort …
**84** PUBLICATIONS **2,560** CITATIONS
SEE PROFILE

Published in final edited form as:
*ACS Appl Mater Interfaces*. 2009 April 29; 1(4): 882–887. doi:10.1021/am900008v.

# Evidence for singlet oxygen generation and biocidal activity in photo-responsive metallic nitride fullerene – polymer adhesive films

**D. Michelle McCluskey**[1], **Tiffany N. Smith**[1], **Praveen K. Madasu**[1], **Curtis E. Coumbe**[1], **Mary A. Mackey**[1], **Preston A. Fulmer**[2], **James H. Wynne**[2], **Steven Stevenson**[1], and **J. Paige Phillips**[1,*]

[1] Department of Chemistry and Biochemistry, University of Southern Mississippi, Hattiesburg, Mississippi 39406

[2] Chemistry Division, Naval Research Laboratory, Washington, District of Columbia 20375

## Abstract

The adhesive properties, as measured by bulk tack analysis, are found to decrease in blends of isomerically pure $Sc_3N@I_h$-$C_{80}$ metallic nitride fullerene (MNF) and polystyrene-*block*-polyisoprene-*block*-polystyrene (SIS) copolymer pressure sensitive adhesive (PSA) under white light irradiation in air. Reduction of tack is attributed to the in-situ generation of $^1O_2$ and subsequent photooxidative crosslinking of the adhesive film. Comparisons are drawn to classical fullerenes $C_{60}$ and $C_{70}$ for this process. This work represents the first demonstration of $^1O_2$ generating ability in the general class of metallic nitride fullerenes, ($M_3N@C_{80}$). Additional support is provided for the sensitizing ability of $Sc_3N@I_h$-$C_{80}$ through the successful photooxygenation of 2-methyl-2-butene to its allylic hydroperoxides in benzene-$d_6$ under irradiation at 420 nm, a process which occurs at a comparable rate to $C_{60}$. Photooxygenation of 2-methyl-2-butene is found to be influenced by the fullerene sensitizer concentration and oxygen gas flow rate. Molar extinction coefficients are reported for $Sc_3N@I_h$-$C_{80}$ at 420 nm and 536 nm. Evaluation of the potential antimicrobial activity of films prepared in this study stemming from the in-situ generation of $^1O_2$ led to an observed 1 log kill for select Gram-positive and Gram-negative bacteria.

### Keywords

singlet oxygen; polymer film; PSA; metallic nitride fullerene; adhesive; fullerene; metallofullerene; MNF; $Sc_3N@C_{80}$; antimicrobial; biocidal

## 1. Introduction

The photophysical properties of empty-cage fullerenes (e.g., $C_{60}$, $C_{70}$), their ability to generate singlet oxygen, and potential impact on medical applications have been well-documented.[1–14] This phenomenon is not limited to classical empty-cage structures, as several other types of fullerenes have emerged recently with the capacity to sensitize the formation of singlet oxygen. In 2001, members of the azafullerene fullerene family, e.g., $(C_{59}N)_2$ and $C_{59}NH$, joined classical empty-cage fullerenes in reports of singlet oxygen formation,[15,16] but with about half the efficiency of $C_{60}$. In the same year, several classical endohedral metallofullerenes (EMFs),

*Address correspondence to Dr. J. Paige Phillips, Department of Chemistry and Biochemistry, University of Southern Mississippi, 118 College Drive, Hattiesburg, Mississippi 39406; Phone: (601) 266-4083; Fax:(601) 266-6075; Janice.Phillips@usm.edu.

e.g., $Dy@C_{82}$ and $Gd@C_{82}$, were also shown to generate singlet oxygen and efficiently sensitize the photooxidation of olefins in an ene reaction.[17] Often this ene reaction is used as a diagnostic tool for the generation of singlet oxygen, where the detection of photooxygenated products is attributed to the singlet oxygen mediated process.[18–21] EMFs have generated a great deal of excitement over their empty-cage cousins, as the inclusion of a metal or metals within the fullerene cage offers increased potential resulting from the unique properties of the encapsulated metal. Possible applications under development include their use in optoelectronic devices and energy conversion systems.[17] Metallic nitride fullerenes, MNFs, e.g. $Sc_3N@C_{80}$ and $Gd_3N@C_{80}$, represent an even more recent addition to the metallofullerene class of compounds, and are characterized by the incorporation of a metal-nitride complex, $M_3N$, inside an all carbon $C_{80}$ cage. Although, there have been no literature reports of singlet oxygen generation from this class of compounds, other application areas which are discussed include their use as MRI contrast agents[22,23] and in photovoltaic devices.[24]

A consequence of the ability of $C_{60}$ to generate singlet-oxygen is the development of new application areas such as fullerene-based, antimicrobial agents. Kai *et al.*[8] have demonstrated the antibacterial activity of $C_{60}$ dissolved with poly(vinylpyrrolidone) K30. Fang *et al.*[25] have shown the effect of $C_{60}$ on both Gram-negative and Gram-positive bacteria in terms of their phospholipid composition. Lyon *et al*[26–28] have described the antibacterial activity of fullerene water suspensions, and Li *et al.*[29] provide an overview of antimicrobial nanomaterials such as $C_{60}$ for water disinfection and microbial control. One of the central technical efforts of our fullerene-polymer research has been the study of how to incorporate metallofullerene nanomaterials into macrostructures (e.g. dendrimers, polymers, films, devices) and exploit their benefits as multi-functional, and in many cases, stimuli-responsive materials, for example, MRI active + antimicrobial.

Polymer blends and crosslinked networks containing fullerene nanomaterials may have potential for use in photovoltaic cells,[30–32] non-linear optical devices,[33–36] and as oxygen sensors.[37] Our group's research interests lie in discovering the unique properties of polymer-nanocomposite structures containing fullerene-based nanomaterials. In this effort, we recently reported the chemical, mechanical, and adhesive properties of interesting stimuli-responsive nanocomposites prepared from rubber-based, pressure sensitive adhesive (PSA) – $C_{60}$ fullerene blends.[38,39] PSAs are widely utilized in commercial tape, label manufacturing, and medical adhesives, and may be produced to have a variety of chemical compositions, such as acrylic, silicone, and rubber-based.[40] Rubber-based systems are typically highly flexible and elastic, and the polystyrene-*block*-polyisoprene-*block*-polystyrene (SIS) copolymer is an example of a commonly applied thermoplastic elastomer-based PSA.[41] These block copolymers have high cohesive strength due to the physical crosslinking, which results from the microphase separation of the hard, high $T_g$, polystyrene segments from the rubbery portions derived from the unsaturated polyisoprene center blocks.[42]

Our group has demonstrated that the adhesive properties of rubber-based elastomeric adhesives, such as SIS, can be dramatically affected when blended with common photochemical sensitizers for the formation of singlet oxygen, including rose bengal, acridine, and $C_{60}$ fullerene.[38,39] The photochemical efficiency of a photosensitizer to generate singlet oxygen is the singlet oxygen quantum yield, $\Psi_{\Delta}$, and is reported to be high (0.8 – 1) for acridine, rose bengal, and $C_{60}$ fullerene in common solvents at visible wavelengths.[3–7,21] Solubility variations, knowledge of singlet oxygen quantum yields, and wavelength dependent absorption extinction coefficients as solid film constituents limited detailed direct comparisons; however, $C_{60}$ fullerene was consistently the superior singlet oxygen generator as measured by a subsequent loss in adhesion of our nanocomposite systems. Purge gas experiments confirmed that the presence of oxygen was essential to the mechanism of adhesive loss, and in combination

with the effects of added singlet oxygen generators and scavengers, these results supported a singlet-oxygen mediated process.

As part of our continuing interest in discovering the unique properties of polymer-nanocomposites containing fullerene-based nanomaterials, we have extended this photochemical study to include isomerically purified $Sc_3N@I_h$-$C_{80}$, Figure 1, and evaluated its ability to produce singlet oxygen in solution and polymer films. This behavior, when extended to other MNF species, has the potential to produce a unique family of stimuli-responsive materials containing functional metals. These MNF-polymer nanocomposite films may hold promise for photovoltaic, photonic, electronic, and biomedical applications. With regard to specific applications, the films produced in this study were evaluated for potential antimicrobial activity resulting from the in-situ generation of singlet oxygen.

## 2. Experimental Section

### Materials

Triblock polymer SIS (D1161) was provided by Kraton Polymers, Inc. (Belpre, Ohio) and was comprised of ~15 wt % polystyrene stabilized with 0.14 wt % Irganox 565 antioxidant. GPC analysis yielded $M_w$ fractions of 315,800 (64 %) and 102,500 (36 %) and polydispersities of 1.08 and 2.45. Toluene (>99.9 % HPLC grade), $d_6$ benzene (>99 %) and 2-methyl-2-butene (>99.5 %) were purchased from Sigma Aldrich. $C_{60}$ and $C_{70}$ were purchased from MER Corporation (Tucson, AZ). The production, separation, and isolation of isomerically pure (> 99 %) $Sc_3N@I_h$-$C_{80}$ used in this study was performed by our new, non-chromatographic purification method as previously described.[43,44] Unless otherwise indicated, all materials were used as received without further purification.

### Photochemical Studies, Solution

Solutions for photochemical studies were prepared by adding a catalytic amount of the fullerene sensitizer, $C_{60}$ or $Sc_3N@I_h$-$C_{80}$, to benzene-$d_6$ solvent with brief sonication to dissolve solids. The 2-methyl-2-butene was added to the sensitizer solution, which was then transferred to a 250 mL, borosilicate glass jacketed photochemical reaction vessel (Ace Glass Inc.). Irradiation was conducted using a Rayonet photochemical reactor fitted with seven, 420 nm $\lambda_{max}$ bulbs. Reaction temperature was maintained at 15 °C by use of a circulating chiller, which was connected to the jacketed portion of the reaction vessel. The system was purged at a constant rate with dry $O_2$ for 30 minutes prior to initiating exposure and maintained for the duration of the reaction. Aliquots of approximately 0.7 mL were removed from the reaction vessel via syringe and analyzed immediately using a 300 MHz/52 MM Bruker NMR. Peroxide products were reduced in a 1M triphenyl phosphine solution for safe handling and disposal. Molar extinction coefficients were determined for fullerene sensitizers through Beer's Law plots of a serially diluted $7.75 \times 10^{-5}$ M $C_{60}$ or $Sc_3N@I_h$-$C_{80}$ starting solution followed by UV/VIS analysis on a Shimadzu UV-2401PC Spectrometer.

### Photochemical Studies, Film Preparation and Bulk Tack Analysis

SIS polymer was dissolved in a toluene solution containing $C_{60}$ or $C_{70}$ fullerenes or $Sc_3N@I_h$-$C_{80}$ MNF and stirred overnight in the dark to prevent early exposure to light. Using an eight-path wet film applicator (Paul N. Gardner Company, Inc.), bulk tack samples were drawn on Q-panel brand test panels from 20 wt % solid solutions in toluene, followed by solvent evaporation in a dark hood overnight. The prepared films averaged 25–30 μm thickness and were visually uniform. Unless otherwise indicated, film samples were irradiated using a 150 W tungsten/halogen white light source. The radiation intensity was measured at the sample (30 s @ 22 °C) with a "power puck" photometer to give 0.004 W/cm$^2$ visible, and no measurable UV-A, UV-B, or UV-C.

Bulk tack studies were conducted on the TA. XTplus Texture Analyser (Godelming, Surrey, UK). An applied force (35 g) on the one inch round probe tip (57R stainless steel) and a probe insertion speed of 0.1 mm/s gave an insertion depth of 10 % film thickness. The applied force was held for 10 s, and then the probe tip was withdrawn at a constant rate of 0.1 mm/s. The applied mass required to remove the probe tip from the film was obtained in grams per unit time, and the highest point was recorded as the peak tack. The probe tip was cleaned with toluene solvent and dried after each tack experiment.

### Antimicrobial Studies

Sensitizer-containing polymer solutions were prepared as described above and flow coated onto glass microscope slides which were maintained in the dark until the bacterial challenge was conducted. These slides were prepared in triplicate at 0.2 and 1.0 wt % fullerene sensitizer. Control slides were prepared by similarly flow coating SIS polymer solution containing no fullerene sensitizer.

**Bacteria and Media—**Luria-Bertani (LB) media (Difco Laboratories, Detroit, MI) was used as a bacterial growth medium for preparation of bacteria for bacterial challenges and was prepared according to manufacturer's specifications. *Staphylococcus aureus* (ATCC 25923) was used for all Gram-positive bacterial challenges, and *Escherichia coli* (ATCC 25922) was used for all Gram-negative bacterial challenges.

**Bacterial Challenge—**Overnight cultures were grown in LB media, pelleted, and resuspended in 0.5 % saline solution at a concentration of $10^9$ CFU/mL. An aliquot of 20 uL ($10^7$ CFU) of the bacterial suspension was deposited as a liquid droplet using a calibrated pipette onto a 1 $cm^2$ area of each coating. The bacteria were exposed to white light under ambient conditions for 2 h. The coatings were then swabbed with a sterile cotton swab that had been dipped in LB broth to ensure bacteria recovery and then placed in 5 mL of LB broth. The broth was then serially diluted seven times. The dilution series were incubated at 37 ºC for 18 h, after which tubes were visually examined and determined to have growth by the presence of turbidity. Log kill was determined by the following relationship: Log kill = 7 – highest dilution exhibiting bacterial growth.

## 3. Results and Discussion

### Film Photochemical Studies - Bulk Tack Analysis

Our group has found that the bulk tack measurement is capable of not only monitoring the gain or loss in adhesive properties, but also provides mechanistic insight into the chemical species produced during irradiation. For example, as more polar species are produced, such as peroxides, an increase in tack is observed. Using FTIR analysis, peak tacks can be correlated to the production of these reactive peroxide intermediates. A preferred molecular structure of a PSA could be generally described as a network having minimal crosslink density and a sufficiently low plateau modulus to yield a high compliance of the adhesive and good contact with the surface. Extensive chemical crosslinking in the elastic segment results in the increase of the modulus above the Dahlquist's criterion ~$10^5$ Pa. The photochemically altered polymer adhesive films therefore exhibit more glassy behavior, and tack is reduced.

Figure 2 illustrates the changes in the adhesive bulk tack as a function of fullerene sensitizer identity and visible exposure time in fullerene-SIS composite adhesive films. Bulk tack of control films, prepared without sensitizer, remains relatively unchanged as a function of exposure time, thus negating a significant thermal contribution to the tack measurement. The temperature of test coupons increases approximately 20 °C over the first 30 min of irradiation, using a 150 W tungsten/halogen lamp at 6″ distance from samples to source, and remains

constant thereafter. Incorporation of as little as $2.0 \times 10^{-4}$ mmol sensitizer/gram of polymer leads to dramatic effects on the tack/time adhesive plot. This low concentration of sensitizer – $C_{60}$, $C_{70}$, and $Sc_3N@I_h$-$C_{80}$ – was employed to better discern any differences among the fullerene series and provide relative kinetic details. $C_{60}$ and $C_{70}$ fullerenes possess similar sensitizing ability, when incorporated into SIS films, and the tack/time plot shows the now characteristic parabolic shape just prior to the complete loss of tack. This transient increase in tack has been attributed to the generation and subsequent decomposition of reactive peroxide intermediates during irradiation. When incorporated into SIS adhesive films, isomerically pure $Sc_3N@I_h$-$C_{80}$ does lead to a loss in adhesive tack, however, at a reduced rate relative to $C_{60}$ and $C_{70}$ classical fullerenes. The shape of the $Sc_3N@I_h$-$C_{80}$ tack/time plot is also characteristic of the singlet oxygen mediated process. Knowledge of singlet oxygen quantum yields and wavelength dependent absorption extinction coefficients as solid film constituents are required for direct comparisons; however one can conclude that under these conditions, $Sc_3N@I_h$-$C_{80}$ is less able to productively generate singlet oxygen as measured by polymer-singlet oxygen chemical reactions leading to the loss of adhesive tack.

## Solution Photochemical Studies – Photooxygenation of 2-methyl-2-butene

To provide further support for the ability of $Sc_3N@I_h$-$C_{80}$ to photochemically generate singlet oxygen, solution studies were performed in a photochemical reactor under visible irradiation, using a modified procedure from that reported by Shinohara.[17] In this process, evidence for singlet oxygen generation is detected by the successful photooxygenation of 2-methyl-2-butene to the allylic hydroperoxides shown, Scheme 1. As was observed by Shinohara, this reaction produces a ~1:1 ratio of the two hydroperoxide products 1 and 2. Each species possesses a well-resolved and unique hydrogen chemical shift ($H_a$, 4.93δ; $H_b$, 3.97 δ; and $H_c$, 5.50 δ) in the $^1$H NMR, corresponding to the area of one hydrogen and leading to the ready analysis of reaction mixtures using integration of $^1$H NMR peak areas. The reaction time was optimized at 1 hour to yield ~10 % conversion of starting material and thereby avoiding the appearance of side products resulting from the degradation of peroxide products.

Table 1 summarizes the solution photochemistry of $Sc_3N@I_h$-$C_{80}$ relative to $C_{60}$ fullerene for the photooxidation of 2-methyl-2-butene via in-situ generated singlet oxygen. All reactions are conducted at a 0.3 M concentration of 2-methyl-2-butene using a catalytic amount of fullerene photosensitizer. In the absence of fullerene sensitizer, no detectable products were obtained. However, a significant conversion to hydroperoxide products was observed in the presence of either $C_{60}$ or $Sc_3N@I_h$-$C_{80}$, and given the experimental error associated with our process, little difference between the two types of fullerene sensitizers could be detected. Reducing the photocatalyst by an order of magnitude resulted in a significant decrease in the production of hydroperoxide products. A similar effect was observed by reducing the oxygen purge rate. This is not surprising since the production of singlet-oxygen generated products is expected to depend on the partial pressure of oxygen in the reaction environment.[45]

## Molar Extinction Coefficients

The molar extinction coefficients were determined in toluene solvent for isomerically purified $Sc_3N@I_h$-$C_{80}$ at 420 and 536 nm and are reported in Figure 3, along with $C_{60}$ values for comparison. The wavelength of 420 nm is chosen to coincide with our photochemical lamp emission $\lambda_{max}$. The 536 nm is an approximate lambda max of the $C_{60}$ visible spectrum. Beer's law plots of prepared dilution series produced linear plots, and good correlation values.

Several classical (non-MNF) endohedral metallofullerenes have been investigated as both singlet oxygen generators by Shinohara[17] and as singlet oxygen quenchers by Yanagi.46 An example energy diagram, which describes the interaction between excited state $C_{60}$ fullerene and ground state molecular oxygen, can be approximated by Figure 4. $C_{60}$ is efficiently

converted to the triplet excited state ($^3S^*$) upon UV irradiation, which efficiently sensitizes the formation of singlet oxygen ($^1O_2$) through an energy transfer mechanism. Once generated, singlet oxygen is free to engage in additional molecular reactions. Shinohara found that $Dy_2@C_{2n}$, $Dy@C_{82}$, $Gd@C_{82}$ all successfully generated high yields of photooxidation products of 2-methyl-2-butene, while $La@C_{82}$ produced no reaction.[17] This work was followed recently by Yanagi, who determined the total quenching rate constant (sum of physical and chemical quenching mechanisms) for $La@C_{82}$ and several other fullerenes, and found that $La@C_{82}$ possessed a quenching rate constant comparable to β-carotene.[46] This process was discussed in terms of a combination of energy and charge transfer processes. The triplet state of the metallofullerene should lie slightly higher in energy than the $^1O_2$ energy for an efficient energy transfer mechanism to occur. Our preliminary findings have significant data to support the generation of singlet oxygen from $Sc_3N@I_h$-$C_{80}$, tentatively placing a lower limit on the excited state energy of $Sc_3N@I_h$-$C_{80}$. A continued investigation to measure more accurate rates and efficiencies for $^1O_2$ generation, probe potential quenching mechanisms and chemical reactivity considerations is ongoing.

### Antimicrobial Studies

Films prepared using $C_{60}$ and $Sc_3N@I_h$-$C_{80}$ sensitizers were also evaluated for potential antimicrobial activity stemming from the in-situ generation of $^1O_2$ under white light, and these results are summarized in Table 2. Techniques for biological assays were adapted from previously published reports.[47,48] Biological results for control samples – no sensitizer – afforded no biological activity against the two pathogenic bacteria examined in this study. A small additive effect was observed for fullerene-sensitized films, where $C_{60}$ and $Sc_3N@I_h$-$C_{80}$ provided a 1–2 log kill of both Gram-(+) and Gram-(−) bacteria. Multiple trials of each system were performed, and we suggest that $C_{60}$ is a more active antimicrobial agent in these systems than $Sc_3N@I_h$-$C_{80}$. This finding is consistent with the photochemical film study, where tack measurements showed generation of peroxide intermediates at a later time under identical conditions. Unfunctionalized fullerenes are hydrophobic and therefore insoluble in water, which prevents a direct comparison to solution anti-microbial studies. The ability of fullerenes to generate singlet oxygen is strongly influenced by chemical modification of the cage and other solubilizing procedures. However, a recent article by Markovic *et al.*[5] offers a current review of the photosensitization ability of select fullerenes, such as $C_{60}$, and their potential application as powerful antimicrobial agents.

## 4. Conclusions

In conclusion, we have evaluated the singlet oxygen generating ability of $Sc_3N@I_h$-$C_{80}$ in solution and SIS adhesive films. This work represents the first demonstration of the singlet oxygen generating ability of this family of compounds and the specific photochemical sensitizing ability of $Sc_3N@I_h$-$C_{80}$. The rate of singlet oxygen generation leading to oxidative crosslinking and subsequent loss of tack in adhesive films was slower for $Sc_3N@I_h$-$C_{80}$ than for the classical fullerenes $C_{60}$ and $C_{70}$, which had comparable rates. A reduced relative rate of singlet oxygen production from $Sc_3N@I_h$-$C_{80}$ is further supported by antimicrobial studies. However in solution photochemical studies, where evidence for production of singlet oxygen is supported by the successful photooxygenation of 2-methyl-2-butene to its allylic hydroperoxides, product yields suggested similar sensitization activity for $Sc_3N@I_h$-$C_{80}$ and $C_{60}$.

## Acknowledgments

JPP thanks NSF CHE-0847481 and NIH R15AG028408 (National Institute on Aging). Additional support from the Office of Naval Research (JHW) and NSF CHE-0547988 (SS) is also acknowledged. Graduate Student Fellowships for MAM (NSF GRFP) and CEC (Department of Education, GAANN #P200A060323) are also acknowledged.

## References


1. Arbogast JW, Darmanyan AP, Foote CS, Rubin Y, Diederich FN, Alvarez MM, Anz SJ, Whetten RL. J Phys Chem 1991;95:11.
2. Foote CS. Top Curr Chem 1994;169:347.
3. Guldi DM, Asmus KD. Radiat Phys Chem 1999;56:449.
4. Guldi DM, Prato M. Acc Chem Res 2000;33:695. [PubMed: 11041834]
5. Markovic Z, Trajkovic V. Biomaterials 2008;29:3561. [PubMed: 18534675]
6. Nakamura E, Tokuyama H, Yamago S, Shiraki T, Sugiura Y. Bull Chem Soc Jpn 1996;69:2143.
7. Orfanopoulos M, Kambourakis S. Tetrahedron Lett 1995;36:435.
8. Kai Y, Komazawa Y, Miyajima A, Miyata N, Yamakoshi Y. Fullerenes, Nanotubes, Carbon Nanostruct 2003;11:79.
9. Bensasson RV, Brettreich M, Frederiksen J, Gottinger H, Hirsch A, Land EJ, Leach S, McGarvey DJ, Schonberger H. Free Radical Biol Med 2000;29:26. [PubMed: 10962202]
10. Bosi S, Da Ros T, Castellano S, Banfi E, Prato M. Bioorg Med Chem Lett 2000;10:1043. [PubMed: 10843212]
11. Bosi S, Da Ros T, Spalluto G, Prato M. Eur J Med Chem 2003;38:913. [PubMed: 14642323]
12. Bosi S, Feruglio L, Da Ros T, Spalluto G, Gregoretti B, Terdoslavich M, Decorti G, Passamonti S, Moro S, Prato M. J Med Chem 2004;47:6711. [PubMed: 15615520]
13. Da Ros T, Prato M. Chem Commun 1999:663.
14. Badireddy AR, Hotze EM, Chellam S, Alvarez P, Wiesner MR. Environ Sci Technol 2007;41:6627. [PubMed: 17948818]
15. Tagmatarchis N, Shinohara H. Org Lett 2000;2:3551. [PubMed: 11073642]
16. Tagmatarchis N, Shinohara H, Fujitsuka M, Ito O. J Org Chem 2001;66:8026. [PubMed: 11722200]
17. Tagmatarchis N, Okada K, Tomiyama T, Yoshida T, Kobayashi Y, Shinohara H. Chem Commun 2001:1366.
18. Alberti MN, Orfanopoulos M. Tetrahedron 2006;62:10660.
19. Singleton DA, Hang C, Szymanski MJ, Meyer MP, Leach AG, Kuwata KT, Chen JS, Greer A, Foote CS, Houk KN. J Am Chem Soc 2003;125:1319. [PubMed: 12553834]
20. Stratakis M, Orfanopoulos M. Tetrahedron 2000;56:1595.
21. Tokuyama H, Nakamura E. J Org Chem 1994;59:1135.
22. Chen Z, Fatouros PP, Corwin FD, Broaddus WC, Dorn HC. Neuro-Oncology 2006;8:492.
23. Fatouros PP, Corwin FD, Chen ZJ, Broaddus WC, Tatum JL, Kettenmann B, Ge Z, Gibson HW, Russ JL, Leonard AP, Duchamp JC, Dorn HC. Radiology 2006;240:756. [PubMed: 16837672]
24. Pinzon JR, Plonska-Brzezinska ME, Cardona CM, Athans AJ, Gayathri SS, Guldi DM, Herranz MA, Martin N, Torres T, Echegoyen L. Angew Chem Int Ed 2008;47:4173.
25. Fang JS, Lyon DY, Wiesner MR, Dong JP, Alvarez PJJ. Environ Sci Technol 2007;41:2636. [PubMed: 17438827]
26. Lyon DY, Adams LK, Falkner JC, Alvarez PJJ. Environ Sci Technol 2006;40:4360. [PubMed: 16903271]
27. Lyon DY, Brunet L, Hinkal GW, Wiesner MR, Alvarez PJJ. Nano Lett 2008;8:1539. [PubMed: 18410152]
28. Lyon DY, Fortner JD, Sayes CM, Colvin VL, Hughes JB. Environ Toxicol Chem 2005;24:2757. [PubMed: 16398110]
29. Li QL, Mahendra S, Lyon DY, Brunet L, Liga MV, Li D, Alvarez PJJ. Water Res 2008;42:4591. [PubMed: 18804836]
30. Barber RP, Gomez RD, Herman WN, Romero DB. Org Electron 2006;7:508.
31. Dennler G, Lungenschmied C, Neugebauer H, Sariciftci NS, Latreche M, Czeremuszkin G, Wertheimer MR. Thin Solid Films 2006;511:349.
32. Janssen RAJ, Hummelen JC, Saricifti NS. MRS Bull 2005;30:33.
33. Antipov OL, Yurasova IV, Domrachev GA. Quantum Electron 2002;32:776.

34. Elim HI, Ji W, Meng GC. J Nonlinear Opt Phys Mater 2003;12:175.
35. Kamanina NV. Synth Met 2003;139:547.
36. Zeng HP, Sun ZR, Segawa Y, Lin FC, Mao S, Xu ZZ. J Appl Phys 2001;89:6539.
37. Amao Y. Microchimica Acta 2003;143:1.
38. Phillips JP, Deng X, Stephen RR, Fortenberry EL, Todd ML, McCluskey DM, Stevenson S, Misra R, Morgan SE, Long TE. Polymer 2007;48:6773.
39. Phillips JP, Deng X, Todd ML, Heaps DT, Stevenson S, Zhou H, Hoyle CE. J Appl Polym Sci 2008;109:2895.
40. Satas, D. Handbook of Pressure Sensitive Adhesive Technology. Status & Associates; Warwick, RI: 1999.
41. Florian S, Novak I. J Mater Sci 2004;39:649.
42. Sung IK, Kim KS, Chin IJ. Polym J 1998;30:181.
43. Stevenson S, Harich K, Yu H, Stephen RR, Heaps D, Coumbe C, Phillips JP. J Am Chem Soc 2006;128:8829. [PubMed: 16819876]
44. Stevenson S, Thompson MC, Coumbe HL, Mackey MA, Coumbe CE, Phillips JP. J Am Chem Soc 2007;129:16257. [PubMed: 18052069]
45. Arai H, Tajima Y, Takeuchi K. Jap J Appl Phys Part 1 2001;40:6623.
46. Yanagi K, Okubo S, Okazaki T, Kataura H. Chem Phys Lett 2007;435:306.
47. Pant RR, Buckley JL, Fulmer PA, Wynne JH, McCluskey DM, Phillips JP. J Appl Polym Sci 2008;110:3080.
48. Wynne JH, Pant RR, Jones-Meehan JM, Phillips JP. J Appl Polym Sci 2008;107:2089. For table of contents use only.

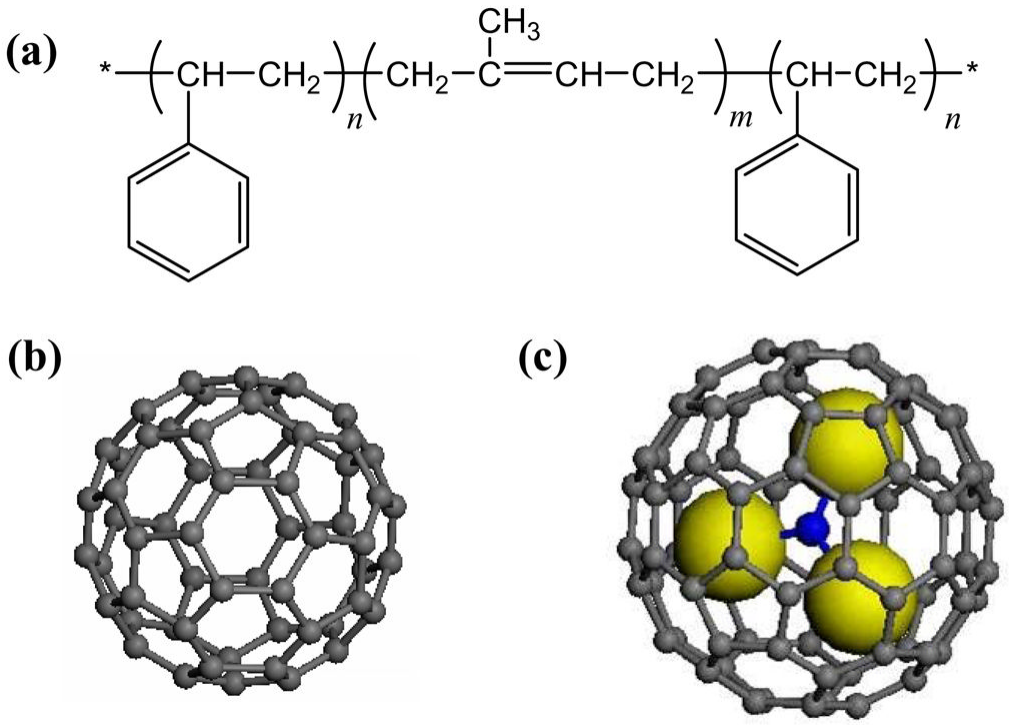


**Figure 1.**
Chemical structures of (a) polystyrene-*block*-polyisoprene-*block*-polystyrene (SIS), copolymer pressure sensitive adhesive (PSA); (b) $C_{60}$ fullerene; and (c) $Sc_3N@I_h$-$C_{80}$ metallic nitride fullerene ($Sc_3$-MNF) sensitizer

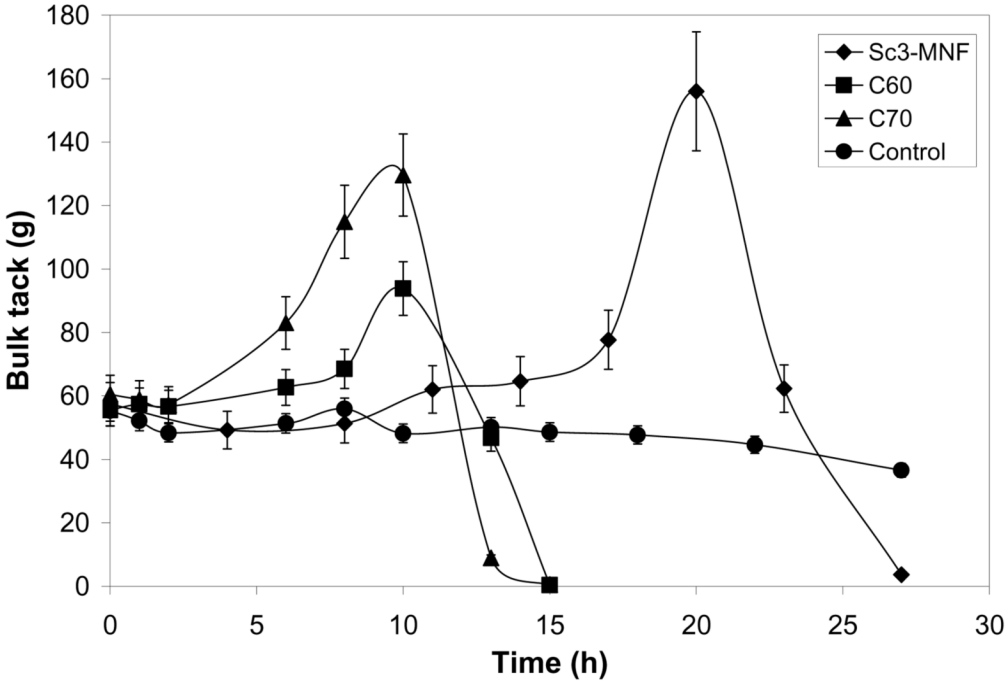


**Figure 2.**

Change in bulk tack of SIS films as a function of fullerene sensitizer identity (e.g., $C_{60}$, $C_{70}$, or $Sc_3N@I_h$-$C_{80}$) and visible irradiation exposure time. Films are prepared containing equal concentrations, $2.0 \times 10^{-4}$ mmol sensitizer/gram polymer and irradiated from 0–30 hr using a 150 W tungsten/halogen light source in air. Each data point represents the average of the peak tack of 5 individual measurements.

**(a)**

| Fullerene | Molar extinction coeff. @ 420 nm | Molar extinction coeff. @ 536 nm |
|---|---|---|
| $C_{60}$ | 827 | 982 |
| $Sc_3$-MNF | 15,800 | 6,600 |

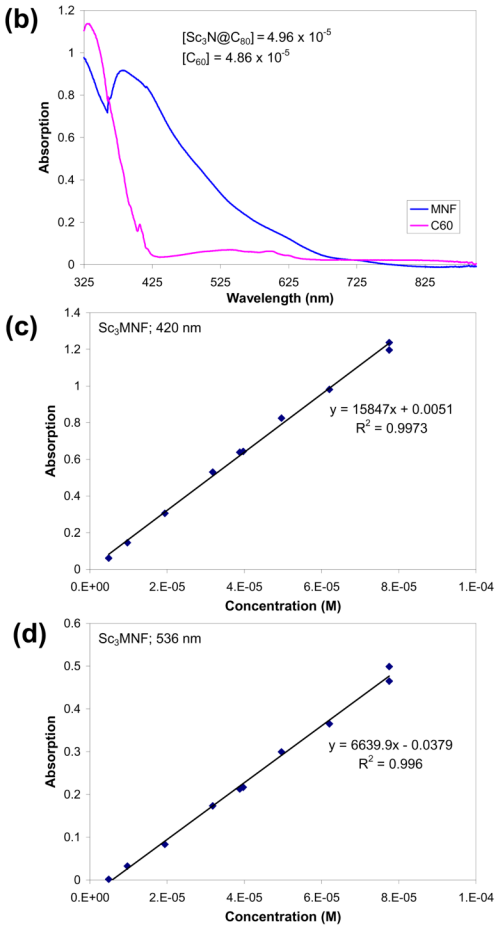


**Figure 3.**

Determination of (a) molar absorptivity coefficients for isomerically purified $Sc_3N@I_h$-$C_{80}$ at 420 and 536 nm using (b) UV-VIS absorption spectra to generate (c, d) Beer's Law plots

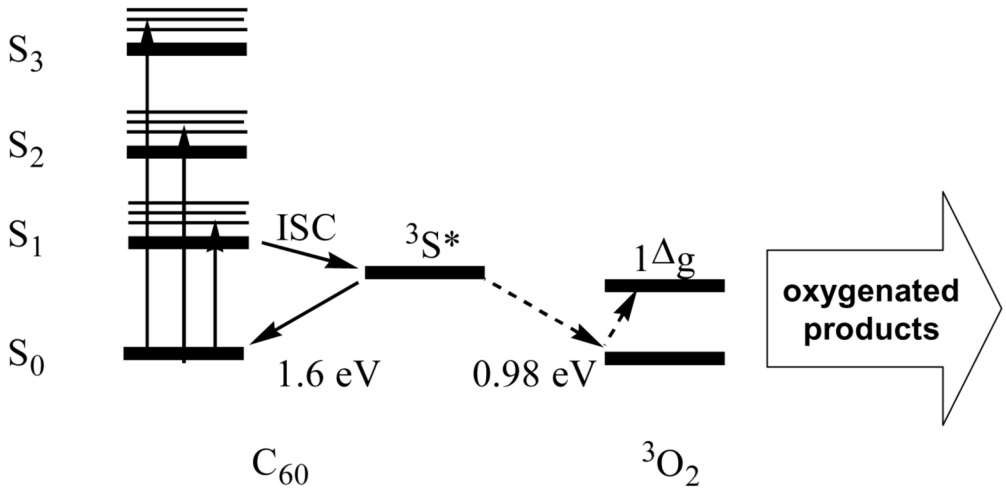


**Figure 4.**
Energy level diagram for the interaction of excited state $C_{60}$ fullerene and ground state molecular oxygen

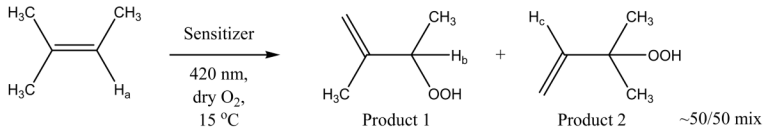


**Scheme 1.**

## Table 1

Ene-photooxygenation of 2-methyl-2-butene with photogenerated singlet oxygen from fullerene sensitizers

| Sensitizer ($C_{60}$ or $Sc_3$-MNF) | Sensitizer concentration (mM) | $O_2$ flow rate[a] (mL/ min) | Conversion[b] %P1 + % P2 |
|---|---|---|---|
| none | none | 120 | 0.0 |
| $C_{60}$ | 0.045 | 120 | 15.6(±1.0) |
| $C_{60}$ | 0.045 | 12 | 6.3(±1.0) |
| $C_{60}$ | 0.0045 | 120 | 5.2(±0.9) |
| $Sc_3$-MNF | 0.045 | 120 | 12.4(±0.6) |
| $Sc_3$-MNF | 0.045 | 12 | 5.1(±0.7) |
| $Sc_3$-MNF | 0.0045 | 120 | 7.0(±1.3) |

[a] $O_2$ flow rate is adjusted using a flow meter prior to irradiation and monitored periodically during the reaction;

[b] % conversion to hydroperoxide products is calculated using $^1$H NMR peak areas, average and (std. dev.) reported for 3 experiments. All experiments were conducted on 0.3 M 2-methyl-2-butene in benzene-$d_6$ solvent and irradiated at 420 nm for 1 hour under an oxygen-rich environment.

**Table 2**

Antimicrobial evaluation of fullerene-containing SIS adhesive films

| Sample ID | Sensitizer Concentration (wt %) | Film testing with *S. aureus*, Gram-(+)[a] | Film testing with *E. coli*, Gram-(−)[a] |
|---|---|---|---|
| SIS control | None | 0 log | 0 log |
| SIS – $C_{60}$ | 0.2 wt% | 1 log | 2 log |
| SIS – $C_{60}$ | 1.0 wt% | 2 log | 2 log |
| SIS – $Sc_3N@I_h$-$C_{80}$ | 1.0 wt% | 1 log | 1 log |

[a] reported in log reduction from a starting concentration of $10^7$ CFU/$cm^2$. Samples were performed in triplicate.